Variability of band alignment between WS$_2$ and SiO$_2$: Intrinsic versus extrinsic contributions Ⓕ✓

Gilles Delie ✉; Peter M. Litwin; Gaby C. Abad; ... et. al

Check for updates

CrossMark

View Online

Export Citation

Related Content

Efficient interlayer electron transfer in a MoTe$_2$/WS$_2$/MoS$_2$ trilayer heterostructure

Appl. Phys. Lett. (June 2021)

Measurement of direct and indirect bandgaps in synthetic ultrathin MoS$_2$ and WS$_2$ films from photoconductivity spectra

Journal of Applied Physics (April 2021)

Reactivity of contact metals on monolayer WS$_2$

Journal of Applied Physics (August 2020)

Variability of band alignment between WS$_2$ and SiO$_2$: Intrinsic versus extrinsic contributions Ⓕ

View Online   Export Citation   CrossMark

Gilles Delie,[1,a] Ⓘ Peter M. Litwin,[2] Gaby C. Abad,[2] Stephen J. McDonnell,[2] Ⓘ
Daniele Chiappe,[3,b] and Valeri V. Afanasiev[1]

AFFILIATIONS

[1]Department of Physics and Astronomy, University of Leuven, 3001 Leuven, Belgium
[2]Department of Materials Science and Engineering, University of Virginia, Charlottesville, Virginia 22904
[3]Imec, Kapeldreef 75, B-3001 Leuven, Belgium

[a]Author to whom correspondence should be addressed: gilles.delie@kuleuven.be
[b]Present address: ASM Microchemistry, Pietari Kalmin katu 3, F 2, 00560 Helsinki, Finland.

ABSTRACT

Internal photoemission of electrons was used to determine the energy position of the top valence band of mono- and few-layer WS$_2$ on an SiO$_2$/Si substrate. It was found, contrary to density functional theory calculations, that the valence band top in WS$_2$ shifts up in energy with respect to the conduction band minimum of SiO$_2$ with decreasing number of monolayers. At the same time, the band alignment of WS$_2$ with SiO$_2$ appears to be less sensitive to the WS$_2$ synthesis route than in the previously studied case of the MoS$_2$/SiO$_2$ interface, indicating less extrinsic WS$_2$ variability.

Published under an exclusive license by the AVS. https://doi.org/10.1116/6.0001987

I. INTRODUCTION

Since demonstration of the first functional two dimensional (2D) transistor by Radisavljevic *et al.*[1] using MoS$_2$ as a channel material, much research has been done on semiconducting transition metal dichalcogenides (TMDs). Initially, mostly, MoS$_2$ was explored, as it showed promising results.[2–5] However, it has been found that synthetically grown MoS$_2$ suffers from significant intrinsic and extrinsic variability. The latter's origin can be correlated with synthesis and processing details of the 2D layers. It has been shown that there is a ≈0.6 eV difference in the band alignment between SiO$_2$ and MoS$_2$ grown by DC magnetron sputtering compared to high temperature sulfurization of metallic molybdenum in H$_2$S, tentatively ascribed to the influence of hydrogen present in the ambient in the last case.[6] Moreover, significant die-to-die threshold voltage (V$_T$) variability has been observed for metal-organic chemical vapor deposition (MOCVD) grown monolayer (ML) MoS$_2$,[7] while few-layer (FL) material seems to be less prone to the V$_T$ variability. Furthermore, layer transfer from a growth- to target-substrate of MoS$_2$ layers grown through high temperature sulfurization of metallic Mo also introduces a significant change in the band alignment with SiO$_2$, causing up to a ≈1 eV energy

difference at edges of the transferred layers, while at the wafer center, the MoS$_2$ valence band (VB) top is shifted by ≈0.5 eV compared to as grown material.[8]

These observations suggest that the variability might be due to a combined action of intrinsic and extrinsic factors. For example, MoS$_2$ thickness variability has been shown to cause degradation of the subthreshold slope (SS). Statistical analysis of 60 devices with a 100 nm channel length shows that MOCVD grown monolayer MoS$_2$ containing islands of a second monolayer results in the SS degradation.[7] Upon further reduction of the channel length, the SS degradation is expected to worsen. The thickness-dependent bandgap width is a well-known intrinsic feature of ML/FL TMDs implying that the gap edges also shift when changing the ML number.[9] This behavior may have a profound effect on electron transport because synthetic TMD layers grown on a wafer scale often contain regions with thicker FL "islands," leading to local gap narrowing.[10] As a result, trapping of charge carriers in these inhomogeneities may significantly impair their transport because the capture cross section becomes comparable to the island size. However, little experimental information is available regarding the VB shift and conduction band (CB) edges upon a TMD film thickness change.

Recently, ML and FL WS$_2$ emerged as a more promising candidate for the use in ultrathin channel transistors since it exhibits a higher electron mobility[11] and provides a better on/off current ratio[12] compared to MoS$_2$-based devices. WS$_2$ also exhibits improved variability of the layer transfer process in terms of energy band alignment with industry standard insulator SiO$_2$.[13] Additionally, we previously noticed that sensitivity to the presence of hydrogen during TMD synthesis might have less of an effect on the WS$_2$ band alignment.[14] Therefore, in this present study, we addressed the intrinsic band alignment variability using internal photoemission (IPE) spectroscopy to determine the energy band alignment of ML and FL WS$_2$ grown though molecular beam epitaxy (MBE) on SiO$_2$. This is achieved by observing optically excited electron transitions from the WS$_2$ VB into the CB of SiO$_2$, which allows one to determine the energy barrier between two bands. Unexpectedly, we found an opposite trend in the case of WS$_2$ compared to MoS$_2$.[6] The WS$_2$ VB top shifts upward in energy relative to the SiO$_2$ CB when decreasing the film thickness from 7 to 1 ML. Additionally, the extrinsic effects were investigated by comparing the hydrogen free MBE synthesis to the WS$_2$ films grown by chemical vapor deposition or sulfurization of metallic tungsten in H$_2$S. By contrast to the earlier studied MoS$_2$ case, we found a negligible impact of hydrogen on the energy band alignment with SiO$_2$. This would point to WS$_2$ as a promising TMD for wafer-scale integration.

II. EXPERIMENTAL DETAILS

A set of 1, 3, 5, and 7 ML thin WS$_2$ films was grown by MBE on top of SiO$_2$ (50 nm)/p-Si(100) substrates at 480 °C with a S to W flux ratio of ≈5000:1. After deposition, the films were left at the growth temperature for 2 min and then allowed to cool down in a continuous S flux. These WS$_2$ layers were *in situ* capped with a ≈5 nm layer of amorphous Se to prevent oxidation in air. The number of MLs were calculated from the physical thickness (0.5, 1.9, 3.7, and 4.8 nm) determined by post growth X-ray photoelectron spectroscopy (XPS) attenuation analysis of the Si 2p core level assuming a 0.7 nm WS$_2$ ML thickness found in the literature.[15,16] The ML sample 0.5 nm thickness has to be interpreted as partial coverage of the substrate. An effective attenuation length (EAL) for the Si 2p$_{3/2}$ core level in the WS$_2$ overlayer was calculated to be 2.30 nm using the NIST electron EAL database.[17] More details of the system used for the MBE growth of WS$_2$ can be found elsewhere.[18] The set of studied samples was complemented by 1 ML WS$_2$ films synthesized on top of similar SiO$_2$/Si substrates by MOCVD from W(CO)$_6$ and H$_2$S precursors at 800 °C using the same approach as described in Ref. 10 as for MoS$_2$. On top of the WS$_2$ films large area optically semitransparent Al and Au electrodes (15 nm thick, 0.5 mm^2) were thermoresistively evaporated to minimize possible damage to the 2D films.[19,20] For the backside contact to the Si substrate wafer, a blanket Al layer was used.

IPE measurements were carried out at room temperature using a 150 W xenon arc lamp as light source in combination with a monochromator (spectral resolution of 2 nm) providing photons in the energy $h\nu$ range from 2 to 6 eV. In the biased WS$_2$/SiO$_2$/Si capacitors, currents were measured under illumination and in darkness using a Keithley 6517a electrometer. The photocurrent was

then determined as the difference between these currents, and by normalizing it to the xenon lamp's calibrated incident photon flux at given photon energy $h\nu$, the quantum yield Y($h\nu$) was determined. By implementing a time delay between the start of illumination and the current readout, transient effects were minimized. Extensive averaging (>60 per current readout) was applied in order to improve the signal-to-noise ratio. Powell's model[21] was used to analyze spectral dependencies of the quantum yield. In order to determine the IPE spectral threshold energy Φ_e, the quantum yield in the region above Φ_e can be approximated as a power function of the photon energy $h\nu$,[21]

$$Y(h\nu) = A(h\nu)(h\nu - \Phi_e)^p, \quad (1)$$

where A($h\nu$) depends on the optical properties of the illuminated sample, including the possible optical interference effects and variations of optical properties of the constituent materials. This factor is usually assumed not to vary significantly within the narrow spectral range above the spectral threshold since no abrupt variations of the optical behavior are expected for the materials in the stack.[21] The exponent p is determined by the excited electron energy distribution in the emitter. As in this case, the VB of WS$_2$ is the emitter and the CB of SiO$_2$ the collector, p is expected to be close to 3, corresponding to a linear increase of the density of states with energy below the semiconductor VB top edge.[21] Indeed, such a linear increase has been directly observed in x-ray photoelectron spectroscopy VB spectra of 1 ML WS$_2$ within approximately the 1 eV range below the VB top.[22] Therefore, the IPE spectral threshold energy Φ_e corresponding to the minimal energy required for an electron to be excited from the WS$_2$ VB top edge into the CB of the underlying SiO$_2$ insulator can be found by linearly fitting the quantum yield spectral curve in Y$^{1/3}$-$h\nu$ coordinates, also known as Powell coordinates.[21] Finally, to account for the image-force barrier lowering effect,[21] spectral thresholds determined at various externally applied gate bias voltages V$_g$ are plotted in $\Phi_e - \sqrt{F}$ coordinates (the Schottky plot). These are then linearly extrapolated to a zero electric field F, determined by normalizing V$_g$ to the oxide thickness, to obtain the interface barrier height.[19]

III. RESULTS AND DISCUSSION

First, we examined the die-to-die consistency of the results to ensure reproducibility of the MBE growth. Figure 1 compares the between yield spectra of two 7 ML WS$_2$ MBE grown samples from different growth runs. Both IPE spectra have an onset of photoemission after 3.5 eV and behave similarly at higher energies. However, there is a slight deviation between both curves above $h\nu \approx 4.3$ eV; this can possibly be explained by the small difference in the growth runs. Specifically, sample A was directly grown up to a 7 ML thickness, while sample B was initially grown to 1 ML thickness for *in situ* characterization and continued to 7 ML thickness a day later. As the second sample used a "seed" layer, it might have induced some changes in the morphology, e.g., less/more island formations or grain size differences, in sample B compared to A. This might explain the small deviation at higher energies of the IPE spectra. Similarly, an apparent kink is observed at ≈4.75 eV for the spectral curve of sample A, and its origin can be
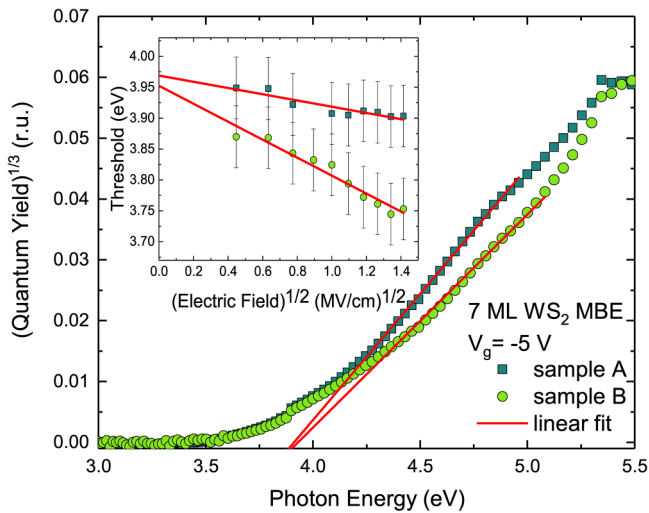
FIG. 1. Powell plots of the IPE quantum yield spectra for two MBE grown 7 ML WS$_2$ samples for a gate bias of -5 V. Red lines indicate the linear fit used to obtain the field-dependent threshold value. The inset shows Schottky plots of the obtained threshold values for both samples, with solid (red) lines indicating the linear fit used to obtain the zero field threshold corresponding to the barrier height between WS$_2$ VB and SiO$_2$ CB. r.u., relative units.

found in a morphology difference. Given that the observed IPE quantum yield spectrum is sensitive to the density of states below the VB top, changes in morphology might induce variations in the WS$_2$ density of states. Nevertheless, the IPE threshold values inferred from the Schottky plot, shown in the inset of Fig. 1 for both samples, have a close zero field threshold values of 4.0 ± 0.1 eV with the SiO$_2$ CB. The thresholds were inferred through linear fitting of the spectral curves at various gate biases over an ≈ 1 eV region above the spectral threshold according to XPS valence band emission spectra, indicating a 1 eV linear increase in the occupied electron state density below the VB top.[22] The difference between the two slopes of the Schottky plots for two samples suggests a difference in built-in electric fields at the WS$_2$/SiO$_2$ interface. Nevertheless, the zero field threshold values remain consistent and can be used to trace the potential sources of the band alignment variations.

Given that MBE synthesis delivers a consistent die-to-die band alignment of WS$_2$ with SiO$_2$, it allows for the direct comparison between ML and FL WS$_2$. Figure 2 shows Powell plots for samples with 7, 5, 3, and 1 ML WS$_2$ films for a range of gate biases. An obvious difference between the spectra is the decreased quantum yield for a decreasing number of layers, a direct result of the difference in the photoexcited WS$_2$ volume. This is a straightforward indication that the observed IPE spectra are the result of electron photoemission from the WS$_2$ films. The intensity difference between 3 and 7 ML is similar to the earlier reported IPE intensity difference between 3 and 6 ML WSe$_2$,[14] while the intensity difference between 1 and 3 ML is larger than the 5–7 ML transition; it is not unexpected as the transition from ML to FL leads to a larger relative difference in the film thickness. It needs to be pointed out

that the Se cap has no influence on the IPE spectra as the photoemission onset of 5 nm Se occurs at a higher energy than observed for these WS$_2$ films.[14] It was already proven that the metal contact (Al versus Au) has no significant influence on the IPE spectra,[14] suggesting that the observed IPE spectra in Fig. 2 originate from the WS$_2$ films.

While the IPE spectra in Fig. 2 have a similar shape, the photoemission onset in the 7 ML WS$_2$ sample is somewhat different than observed for the other WS$_2$ film thicknesses. We already reported a similar difference in the onset of a photoemission shape for 3 and 6 ML WSe$_2$ (cf. Fig. 6 in Ref. 14). This similarity between two WX$_2$ (X = S, Se) films probably indicates an intrinsic property of the valence band top edge in the transition from a 2D layer to a more bulklike material. Nevertheless, the energy onset of photoemission appears to be similar in energy for all FL WS$_2$ films as indicated by the red lines in Fig. 2. All the inferred field-dependent spectral threshold values are combined in the Schottky plot shown in Fig. 3. Linear extrapolation to zero field of the FL WS$_2$ spectral threshold results in a zero field threshold of 4.0 ± 0.1 eV for 5 and 7 ML. Meanwhile, the 3 ML sample has a slightly higher threshold, but it falls within the margin of error as compared to other FL films. These results are consistent with the band structure evolution of WS$_2$, which is not expected to change significantly with the film thickness between 3 and 7 MLs.[9] By contrast, the noticeable IPE threshold shift is observed upon transition from FL to ML WS$_2$, indicating a change in the band alignment between WS$_2$ and SiO$_2$. The zero field threshold obtained for 1 ML WS$_2$ is 3.8 ± 0.1 eV, which is approximately 0.2–0.3 eV lower in energy compared to FL WS$_2$, indicates an up-shift of the VB top for the FL to ML transition as schematically illustrated in Fig. 4. This up-shift trend is opposite to what has been observed for the band alignment of MoS$_2$ with SiO$_2$.[6] Not only is the trend for WS$_2$ opposite to that of MoS$_2$, it is also opposite to density functional theory (DFT) calculations of WS$_2$ films.[23–25] These predict that with increasing number of layers, the valence band moves up in energy. It needs to be pointed out, however, that these calculations are based on freestanding films, while these experimental results are obtained from films on Si/SiO$_2$ substrates. Earlier, we reported on the failure of DFT to correctly predict the band alignment of WS$_2$ versus WSe$_2$ with SiO$_2$.[14] Therefore, while DFT calculations might be correctly predicting the band structure evolution over different thicknesses, there are some discrepancies when the film is supported by a substrate. Knowing that experimental results on WS$_2$ band alignment with SiO$_2$ have been different in terms of predicted relative positions for two separate experiments compared to DFT calculations, there is a possible, e.g., electrostatic interaction of WS$_2$ with the SiO$_2$ substrate, which has not been observed for MoS$_2$. The latter trend for MoS$_2$ thickness-dependent VB positions follows well the trend predicted by DFT calculations. The unexpected result for WS$_2$ suggests that care has to be taken when assessing the origins of device variability, as island formations causing SS degradation as observed for MoS$_2$[7] might not be the same for other semiconductors from the TMD group.

Keeping in mind that the extrinsic synthesis variability observed for MoS$_2$[6] is possibly caused by the presence of hydrogen during TMD film growth, a similar investigation was performed on WS$_2$ layers. We compared these MBE (intrinsically hydrogen free
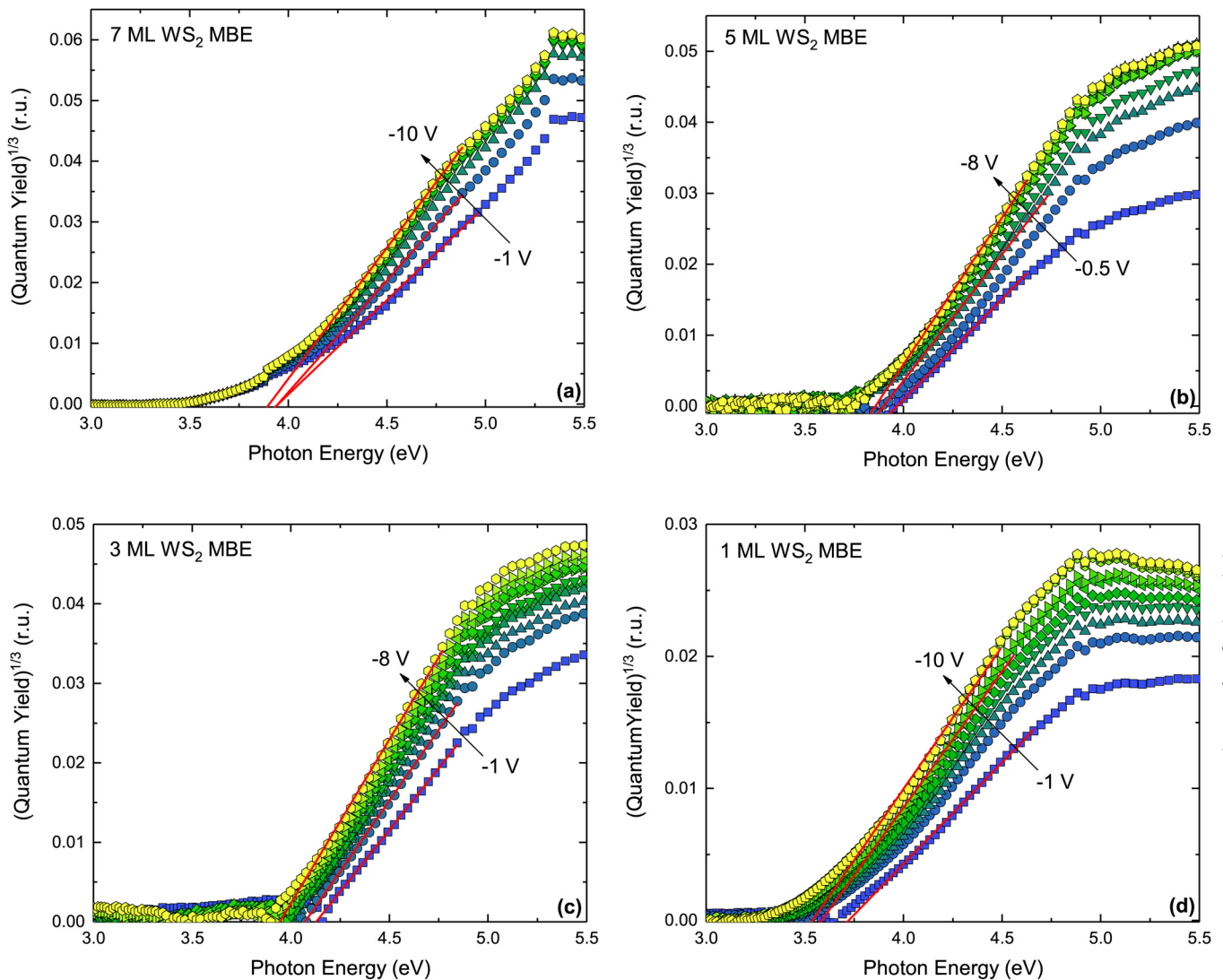
**FIG. 2.** Powell plots of the IPE quantum yield spectra for MBE grown (a) 7, (b) 5, (c) 3, and (d) 1 ML WS$_2$ films for gate biases ranging between -0.5 and -10 V. Solid (red) lines illustrate the linear fit used to obtain the field-dependent threshold values.

process) grown films to earlier reported band alignment values for 4 ML WS$_2$ synthesized on SiO$_2$ by sulfurization of metallic W in H$_2$S at 800 °C.[26] Figure 5 compares the IPE spectra for 5 ML WS$_2$ grown by MBE with a 4 ML film grown by W sulfurization taken at the WS$_2$ gate bias of -5 V. These spectra are in remarkable agreement with each other, both in terms of intensity and the energy onset of photoemission. Nevertheless, a slight decrease of intensity is observed for the 4 ML sample, but that is to be expected for a decreased number of layers. This resemblance is also reflected in the zero field threshold of 4.0 ± 0.1 eV obtained from the Schottky plot shown in Fig. 3. This result is a first indication of a limited extrinsic variability of the band alignment of WS$_2$ caused by the
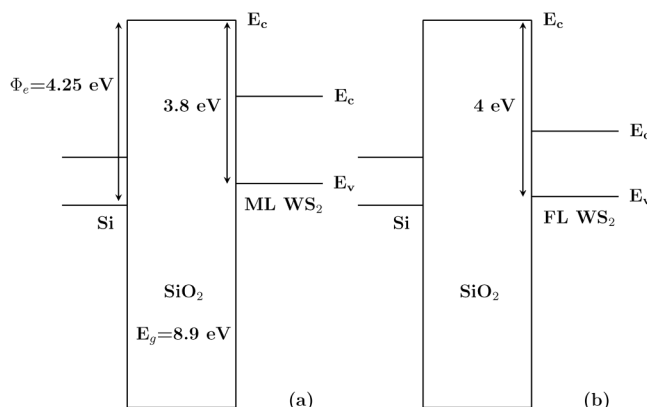
change of the synthesis method. On the other hand, comparing IPE yield spectra for MBE- and MOCVD- grown 1 ML WS$_2$ in Fig. 6 reveals a slight increase of the spectral threshold for the latter. However, the Schottky plots shown in Fig. 3 yield close zero field threshold values for both synthesis methods of ML WS$_2$ at 3.8 ± 0.1 eV. The change in the Schottky plot slope for the MOCVD grown film suggests introduction of charges to the interface probably associated with the presence of hydrogen in the synthesis ambient. Earlier, we already demonstrated the initial indications of good reproducibility of the MOCVD process for 1 ML materials in terms of band alignment with the Si/SiO$_2$ substrate.[13] However, as the band alignment for all three synthesis
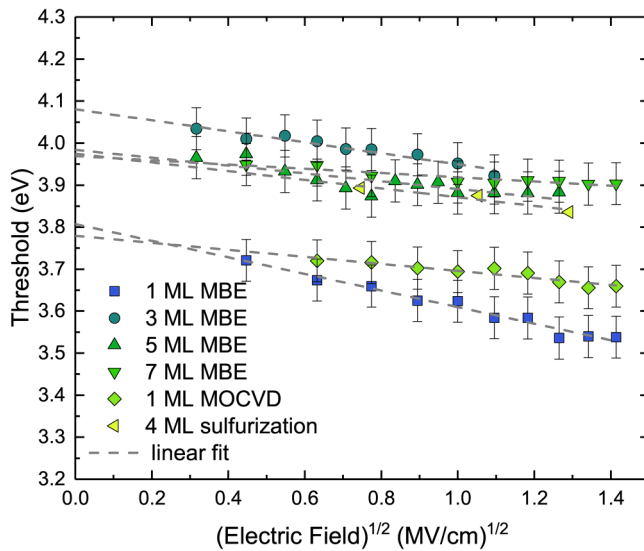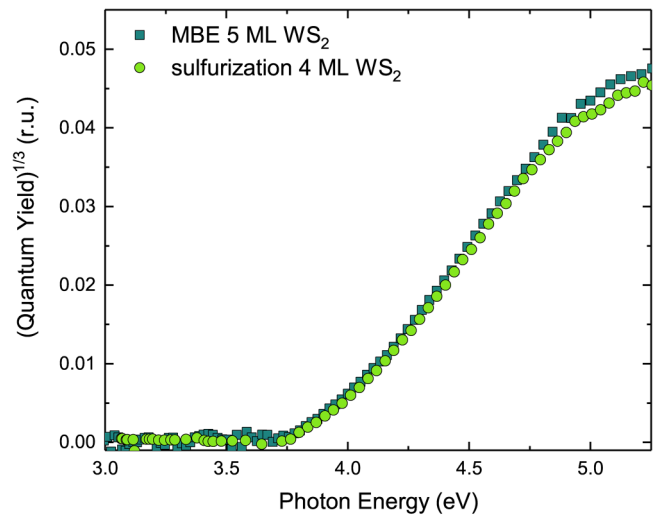
FIG. 3. Schottky plot of the inferred spectral thresholds for MBE grown ML and FL, MOCVD grown ML, and sulfurization grown FL WS$_2$. Dashed gray lines indicate the linear fit used to determine the zero field threshold.

FIG. 5. Comparison between IPE spectra of WS$_2$ grown through MBE (5 ML) and sulfurization (4 ML) with a gate bias of −5 V.

methods discussed above falls within the margin of error of one another, it suggests that the presence of hydrogen during WS$_2$ synthesis might have by far lesser impact on the interface band alignment than in the case of MoS$_2$/SiO$_2$. Together with the earlier reported reduced variability due to the film transfer process,[13] WS$_2$ seems to be less prone to extrinsic variability compared to its MoS$_2$ counterpart. The similarity in threshold values between ML MBE- and MOCVD-grown and FL MBE- and sulfurization-grown allows for the indirect comparison between the MOCVD and sulfurization synthesis. As the same band alignment evolution trend is observed for those synthesis methods, the opposite trend to theoretical
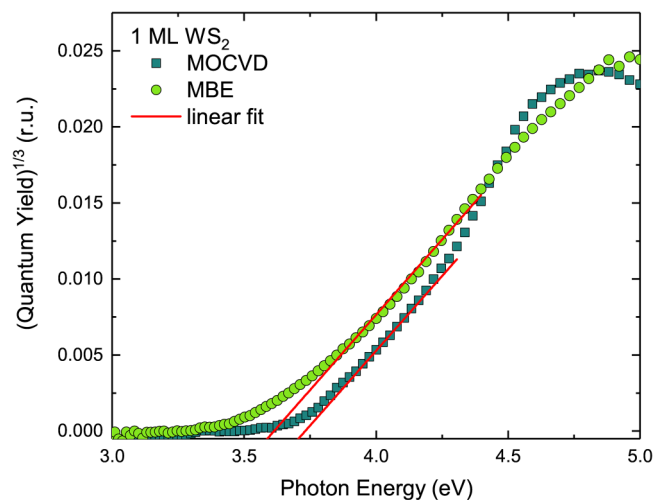
calculations seems to be an intrinsic property of synthetic WS$_2$. Band alignment characterization of exfoliated WS$_2$ materials on SiO$_2$ could reveal if the apparent intrinsic trend is caused by the use of a synthetic material, although to our knowledge, none has been performed up to date. This is probably related to a typically small size of the exfoliated flakes precluding reliable measurements of the IPE current.

Summarizing the above results, one may point to several significant differences in the evolution of WS$_2$/SiO$_2$ band alignment to the earlier studied seemingly similar MoS$_2$/SiO$_2$ systems. First,

FIG. 4. Schematic representation of the energy band alignment of (a) ML and (b) FL WS$_2$/SiO$_2$/Si heterostructures.

FIG. 6. Comparison between IPE spectra obtained from 1 ML WS$_2$ layers grown through MOCVD and MBE with a gate bias of −5 V. Solid (red) lines indicate the linear fit used to determine the spectral threshold values.

the intrinsic VB shift with increasing ML number occurs in the opposite direction; i.e., the VB of ML WS_2 is energetically positioned above that of multilayer's as shown in Fig. 4. The effect of the substrate-related artifacts can be considered insignificant since the VB position appears to be the same in the 7 ML samples (A and B). Second, the extrinsic factors related to the WS_2 synthesis route appear to have by far less impact on the band alignment with SiO_2 than in the case of MoS_2.

IV. CONCLUSION

In conclusion, reduced WS_2 extrinsic variability and consistent band alignment with SiO_2 were found for three different synthesis routes, showing less sensitivity to hydrogen presence during synthesis than in the previously studied case of the MoS_2/SiO_2 interface. At the same time, for intrinsic WS_2 variability, an unexpected trend was found as the valence band top in WS_2 shifts up in energy with decreasing number of monolayers as measured with respect to the conduction band minimum of SiO_2. This would make localization of holes in the islands of larger thickness energetically unfavorable and deliver higher hole mobility in the inhomogeneous layers. Therefore, WS_2 might be a more suitable material for p-channel devices than MoS_2. Taken together with higher electron mobility, WS_2 seems to be the TMD of choice for complementary MOS device integration.

AUTHOR DECLARATIONS

Conflict of Interest

The authors have no conflicts to disclose.

Author Contributions

Gilles Delie: Conceptualization (equal); Data curation (equal); Formal analysis (equal); Investigation (equal); Methodology (equal); Writing – original draft (lead). **Peter M. Litwin:** Methodology (equal); Writing – review & editing (equal). **Gaby C. Abad:** Methodology (equal); Writing – review & editing (equal). **Stephen J. McDonnell:** Funding acquisition (equal); Project administration (equal); Writing – review & editing (equal). **Daniele Chiappe:** Methodology (equal). **Valeri V. Afanasiev:** Funding acquisition (equal); Investigation (equal); Project administration (equal); Writing – review & editing (equal).

DATA AVAILABILITY

The data that support the findings of this study are available from the corresponding author upon reasonable request.

REFERENCES

[1] B. Radisavljevic, A. Radenovic, J. Brivio, V. Giacometti, and A. Kis, Nat. Nanotechnol. **6**, 147 (2011).
[2] H. Wang *et al.*, Nano Lett. **12**, 4674 (2012).
[3] S. Das, H.-Y. Chen, A. V. Penumatcha, and J. Appenzeller, Nano Lett. **13**, 100 (2013).
[4] S. B. Desai *et al.*, Science **354**, 99 (2016).
[5] J. Wang *et al.*, Adv. Mater. **28**, 8302 (2016).
[6] I. Shlyakhov, J. Chai, M. Yang, S. Wang, V. V. Afanas'ev, M. Houssa, and A. Stesmans, APL Mater. **6**, 026801 (2018).
[7] Q. Smets *et al.*, *2020 IEEE International Electron Devices Meeting* (IEEE, New York, 2020), p. 3–1.
[8] V. Afanas'ev, D. Chiappe, M. Perucchini, M. Houssa, C. Huyghebaert, I. Radu, and A. Stesmans, Nanotechnology **30**, 055702 (2018).
[9] I. Tanabe *et al.*, Appl. Phys. Lett. **108**, 252103 (2016).
[10] D. Chiappe *et al.*, Nanotechnology **29**, 425602 (2018).
[11] A. Rawat *et al.*, J. Mater. Chem. A **6**, 8693 (2018).
[12] T. Georgiou *et al.*, Nat. Nanotechnol. **8**, 100 (2013).
[13] G. Delie, D. Chiappe, I. Asselberghs, C. Huyghebaert, I. Radu, S. Banerjee, B. Groven, S. Brems, and V. V. Afanas'ev, Nano Express **2**, 024004 (2021).
[14] G. Delie, P. M. Litwin, S. J. McDonnell, D. Chiappe, M. Houssa, and V. V. Afanas'ev, ECS J. Solid State Sci. **9**, 093009 (2020).
[15] K. Tian, K. Baskaran, and A. Tiwari, Thin Solid Films **668**, 69 (2018).
[16] Y. Yoo, Z. P. Degregorio, and J. E. Johns, J. Am. Chem. Soc. **137**, 14281 (2015).
[17] C. J. Powell *et al.*, "NIST database for the simulation of electron spectra for surface analysis (SESSA)," version 2.1.1, 2018.
[18] K. M. Freedy, P. M. Litwin, and S. J. McDonnell, ECS Trans. **77**, 11 (2017).
[19] V. V. Afanas'ev, D. Chiappe, C. Huyghebaert, I. Radu, S. De Gendt, M. Houssa, and A. Stesmans, Microelectron. Eng. **147**, 294 (2015).
[20] V. V. Afanas'ev, G. Delie, M. Houssa, I. Shlyakhov, A. Stesmans, and V. Trepalin, J. Phys.: Condens. Matter **32**, 413002 (2020).
[21] R. Powell, J. Appl. Phys. **41**, 2424 (1970).
[22] H. Zhu *et al.*, Appl. Phys. Lett. **112**, 171604 (2018).
[23] J. Kang, S. Tongay, J. Zhou, J. Li, and J. Wu, Appl. Phys. Lett. **102**, 012111 (2013).
[24] D. Bocharov, S. Piskunov, Y. F. Zhukovskii, and R. A. Evarestov, Phys. Status Solidi Rapid Res. Lett. **13**, 1800253 (2019).
[25] H.-G. Kim and H. J. Choi, Phys. Rev. B **103**, 085404 (2021).
[26] V. V. Afanas'ev, D. Chiappe, A. Leonhardt, M. Houssa, C. Huyghebaert, I. Radu, and A. Stesmans, ECS Trans. **80**, 191 (2017).